PCCP

PAPER

View Article Online
View Journal | View Issue

Cite this: *Phys. Chem. Chem. Phys.*, 2017, **19**, 21364

Rotationally resolved electronic spectroscopy of the rotamers of 1,3-dimethoxybenzene†

Michael Schneider,[a] Martin Wilke,[a] Marie-Luise Hebestreit,[a] José Arturo Ruiz-Santoyo,[b] Leonardo Álvarez-Valtierra,[b] John T. Yi,[c] W. Leo Meerts,[d] David W. Pratt[e] and Michael Schmitt*[a]

Received 30th June 2017,
Accepted 24th July 2017

DOI: 10.1039/c7cp04401a

rsc.li/pccp

Conformational assignments in molecular beam experiments are often based on relative energies, although there are many other relevant parameters, such as conformer-dependent oscillator strengths, Franck–Condon factors, quantum yields and vibronic couplings. In the present contribution, we investigate the conformational landscape of 1,3-dimethoxybenzene using a combination of rotationally resolved electronic spectroscopy and high level *ab initio* calculations. The electronic origin of one of the three possible planar rotamers (rotamer (0,180) with both substituents pointing at each other) has not been found. Based on the calculated potential energy surface of 1,3-dimethoxybenzene in the electronic ground and lowest excited state, we show that this can be explained by a distorted non-planar geometry of rotamer (0,180) in the S_1 state.

1 Introduction

The investigation of equilibria between conformers or rotamers, which are separated by intermediate barriers ($\approx$5–10 kJ mol^{-1}) and/or have small absolute energy differences ($<$1 kJ mol^{-1}) compared to the thermal energy kT per mol at room temperature ($\approx$2.48 kJ mol^{-1} at 25 °C), has only been made possible by the development of molecular beam techniques.[1,2] The stabilization of selected low energy conformers at the resulting low temperatures in molecular beams, along with the simplification of the spectra due to population of few quantum states at these temperatures, aids in the assignment of observed spectral features to particular molecular species. On the other hand, however, the cooling in molecular beams is far from thermodynamic equilibrium, and different degrees of freedom cool down at individual rates. Mostly, a delicate balance between several factors determines the number and type of conformers observed in a molecular beam, including the energy differences of the conformers, barrier heights, the final temperature in the molecular beam, and the ratio of vibrational to conformational cooling.[3–7]

Here, we focus on the rotamer distribution in three hydroxy and/or methoxybenzenes; 1,3-dihydroxybenzene, 1-hydroxy-3-methoxybenzene, and 1,3-dimethoxybenzene (see Fig. 1; two dihedral angles,‡ defining the orientations of the substituents with respect to the chromophore distinguish the different rotamers of each constitutional isomer). 1,3-Dihydroxybenzene (resorcinol) has been the topic of several experimental and computational studies.[8–13] Using rotationally resolved laser induced fluorescence spectroscopy, two rotamers could be identified in the molecular beam spectra as (180,180)/(0,0) and (180,0).[14] Wilke *et al.*[15] examined the rotamers of 1-hydroxy-3-methoxybenzene and found three different rotamers, namely (180,180), (180,0) and (0,0). Breen *et al.*[16] assigned three vibronic bands in the resonant two-photon ionization (R2PI) molecular beam spectrum of 1,3-dimethoxybenzene at 36101.5, 36163.9, and 36256.9 cm^{-1} to the electronic origins of three different rotamers. Yang *et al.*[17] performed two-color resonant two-photon mass-analyzed threshold ionization spectroscopy to investigate selected rotamers of 1,3-dimethoxybenzene in their cationic states. They found three different ionization potentials for the three lowest-energy bands in the R2PI spectrum of 1,3-dimethoxybenzene from ref. 16 and also concluded the existence of three different rotamers.

[a] *Heinrich-Heine-Universität, Institut für Physikalische Chemie I, D-40225 Düsseldorf, Germany. E-mail: mschmitt@uni-duesseldorf.de; Fax: 49 211 8113689; Tel: 49 211 81 12100*
[b] *División de Ciencias e Ingenierías, Universidad de Guanajuato-Campus León, León, Guanajuato 37150, Mexico*
[c] *Department of Chemistry, Winston-Salem State University, Winston-Salem, North Carolina 27110, USA*
[d] *Radboud University, Institute for Molecules and Materials, Felix Laboratory, Toernooiveld 7c, 6525 ED Nijmegen, The Netherlands*
[e] *Department of Chemistry, University of Vermont, Burlington, Vermont 05405, USA*

† Electronic supplementary information (ESI) available. See DOI: 10.1039/c7cp04401a

‡ Two dihedral angles, which define the orientation of the substituents with respect to the chromophore are selected. Two carbon atoms of the chromophore and both heavy atoms of the individual substituents are needed. The first angle starts at the lowest unsubstituted carbon atom in the benzene ring C(2) and the second one at C(4), so that both angles are formed by C(2)C(1)O(7)C(9) and C(4)C(5)O(8)C(10). For systems with two identical substituents, rotamer (180,180) and (0,0) are equivalent.

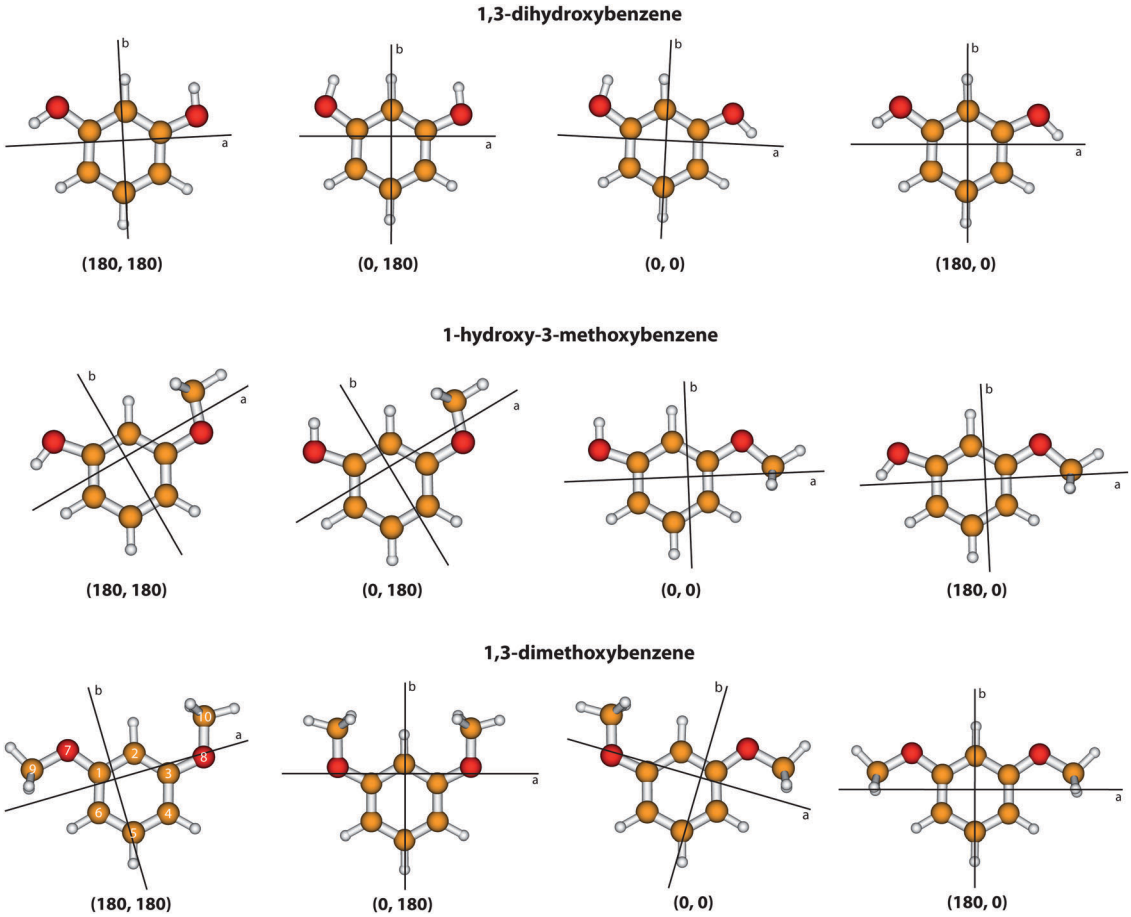

Fig. 1 Structures of the low energy rotamers of 1,3-dihydroxybenzene, 1-hydroxy-3-methoxybenzene, and 1,3-dimethoxybenzene with their main inertial axes. The nomenclature for the rotamers uses the dihedral angles of the hydroxy and methoxy groups, respectively. For details see text.

Surprisingly, rotamer (0,180) has not be observed in molecular beam experiments of 1,3-dihydroxybenzene and 1-hydroxy-3-methoxybenzene, while all structures have been assigned in the case of 1,3-dimethoxybenzene.[16,17] In the present contribution, we use a combination of rotationally resolved electronic spectroscopy and high-level quantum mechanical calculations to investigate the conformational landscape of 1,3-dimethoxybenzene and compare it to that of 1,3-dihydroxybenzene and 1-hydroxy-3-methoxybenzene. In contrast to the results of Breen[16] and Yang,[17] only two of the three conformers could be found and identified. Several reasons for the absence of the missing conformers are discussed.

2 Experimental section

2.1 Experimental procedures

1,3-Dimethoxybenzene (≥98%) was purchased from Sigma-Aldrich and used without further purification. To record rotationally resolved electronic spectra, the sample was heated to 60 °C and co-expanded with 550 mbar of argon into the vacuum through a 200 μm nozzle. After the expansion, a molecular beam was formed using two skimmers (1 mm and 3 mm) linearly aligned inside a differentially pumped vacuum system consisting of three vacuum chambers. The molecular beam was crossed at right angles with the laser beam 360 mm downstream of the nozzle. To create the excitation beam, 10 W of the 532 nm line of a diode pumped solid state laser (Spectra-Physics Millennia eV) pumped a single frequency ring dye laser (Sirah Matisse DS) operated with Rhodamine 110. The output of the dye laser was frequency doubled in an external folded ring cavity (Spectra Physics Wavetrain) with a resulting power of about 5 mW during the experiments. The spectral bandwidth in the UV is 800 kHz. The fluorescence light of the samples was collected perpendicular to the plane defined by laser and molecular beam by an imaging optics setup consisting of a concave mirror and two plano-convex lenses onto the photocathode of a UV enhanced photomultiplier tube (Thorn EMI 9863QB). The signal output was then discriminated and digitized by a photon counter and transmitted to a PC for data recording and processing. The relative frequency was determined using a quasi confocal Fabry–Perot interferometer. The absolute frequency was obtained by comparing the recorded spectrum to the tabulated lines in the iodine absorption spectrum.[18] A detailed description of the experimental setup for rotationally resolved laser induced fluorescence spectroscopy has been given previously.[19,20]

2.2 Quantum chemical calculations

Structure optimizations were performed employing Dunning's correlation-consistent polarized valence triple zeta (cc-pVTZ) basis set from the Turbomole library.[21,22] The equilibrium geometries of the electronic ground and the lowest excited singlet states were optimized using the approximate coupled cluster singles and doubles model (CC2) employing the resolution-of-the-identity approximation (RI).[23–25] Vibrational frequencies and zero-point corrections to the adiabatic excitation energies were obtained from numerical second derivatives using the NumForce script.[26] A natural-bond-orbital (NBO) analysis[27] was performed at the optimized geometries by using the wavefunctions from the CC2 calculations as implemented in the Turbomole package.[28]

Calculations of the potential energy surface (PES) were performed using the Scan keyword in Gaussian 09 package at DFT/B3LYP/cc-pVTZ level of theory.[29] It was built by scanning the two dihedral torsional angles in steps of 5° from 0° to 360°.

2.3 Fits of the rovibronic spectra using evolutionary algorithms

Evolutionary algorithms allow us to make a quick and successful automatic assignment of the rotationally resolved spectra, even for large molecules and dense spectra.[30–33] Beside a correct Hamiltonian to describe the spectrum and reliable intensities inside the spectrum, an appropriate search method is needed. Evolutionary strategies are a powerful tool to handle complex multiparameter optimizations and find the global optimum. For the analysis of the presented high-resolution spectra, we used the covariance matrix adaptation evolution strategy (CMA-ES), which is described in detail elsewhere.[34,35] In this variant of global optimizers mutations are adapted *via* a CMA mechanism to find the global minimum, even on rugged search landscapes that are additionally complicated due to noise, local minima and/or sharp bends.

3 Results

3.1 Computational results

Table 1 summarizes the molecular properties of three low energy rotamers of 1,3-dimethoxybenzene at the CC2/cc-pVTZ level of theory. These are the rotational constants in the ground (A'', B'', C'') and lowest electronically excited (A', B', C') states, their changes upon excitation (ΔA, ΔB, ΔC) and the inertial defects of the respective states (ΔI). Apart from structural parameters, also electronic information such as the orientation of the transition dipole moment (TDM) vector and the adiabatic excitation energy ν_0 are compiled in Table 1.

The TDM-orientation is given by the angle θ of the TDM-vector with the principal inertial *a*-axis. As can be seen from Table 1, the TDM-vectors of rotamer (180,0) and (0,180) are aligned perfectly along the *a*-axis, while that of rotamer (180,180)/(0,0) is rotated by less than 10° towards the *b*-axis. Since the TDM depends on the charge redistribution upon electronic excitation, its orientation can be inferred from the molecular orbitals and the coefficients of the respective excitations that are shown in Fig. 2. For all three possible rotamers, the lowest electronically excited state is dominated by a LUMO ← HOMO excitation with smaller contributions of a LUMO+3 ← HOMO−1 transition and LUMO ← HOMO−1 for rotamer (180,180)/(0,0). From Fig. 2, it becomes clear that the electron density upon excitation is transferred along the inertial *a*-axis which leads to an angle θ of 0° for the highly symmetric rotamers (180,0) and (0,180) within its point group C_{2v}.

Table 1 Molecular properties of the thee possible rotamers of 1,3-dimethoxybenzene at CC2/cc-pVTZ level of theory. For details see text

	(180,180)/(0,0)	(180,0)	(0,180)
A''/MHz	2539	3486	1892
B''/MHz	893	771	1108
C''/MHz	666	636	705
$\Delta I''$/μÅ^2	−6.40	−6.40	−6.41
A'/MHz	2482	3358	1863
B'/MHz	880	763	1091
C'/MHz	655	626	695
$\Delta I'$/μÅ^2	−6.42	−6.42	−7.44
ΔA/MHz	−57	−128	−29
ΔB/MHz	−13	−8	−17
ΔC/MHz	−11	−10	−10
θ/°	6	0	0
ν_0/cm^{-1}	36 809	36 986	36 455

The CC2-calculated relative energies of the possible rotamers, the barriers separating the different rotamers and the adiabatic excitation energies from the ground to lowest electronically excited singlet state are shown in Fig. 3.

The rotamers (180,180) and (0,0) are equivalent and therefore have the same energy, which is the lowest in the electronic ground state of all possible rotamers of 1,3-dimethoxybenzene. Rotating one of the methyl groups by ±180° leads to a destabilization of 226 cm^{-1} for rotamer (0,180) and 188 cm^{-1} for rotamer (180,0). In the lowest electronically excited state, rotamer (0,180) is the more stable one and (180,0) the less, with an energy gap of around 500 cm^{-1}. Given these facts, the excitation energies are expected to increase in the order (0,180) < (180,180)/(0,0) < (180,0).

The barriers separating the minima in the ground state were calculated by varying the dihedral angles of the substituent with the chromophore in steps of 10°. Thus, the transition states belong to structures with one of the substituent perpendicular to the chromophore, as it is the case for 2-methoxyphenol[36] and 3-methoxyphenol.[15] The resulting barriers are around 1400 cm^{-1} above the global minimum of rotamer (180,180)/(0,0) and in general agreement with the results from Yang *et al.*[17]

Rotating both substituents simultaneously leads to saddle points in the same energy range as the transition states for the one-dimensional rotation. This is shown in the two-dimensional potential energy surface presented in Fig. 4. The minima and transition states are located at lines that are parallel to the individual coordinates of each of the rotations. Three different paths, which connect the equivalent minima (180,180) and (0,0), are possible. A one-dimensional rotation of one methoxy group along dihedral angle 1 in Fig. 4 leading to rotamer (0,180) is followed by a one-dimensional rotation of the other methoxy

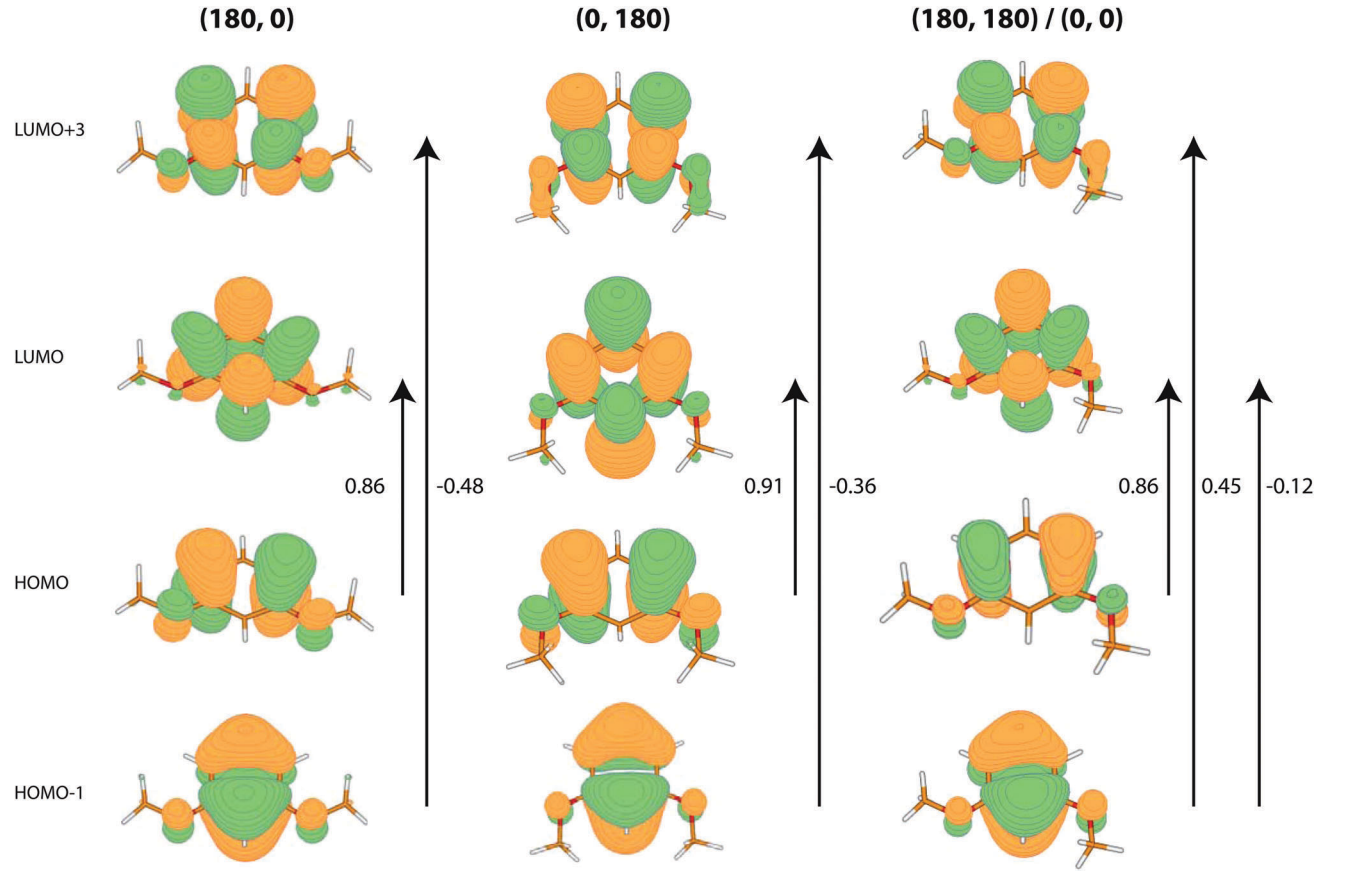

Fig. 2 Frontier orbitals of the different rotamers of 1,3-dimethoxybenzene and the coefficients of the respective excitations according to CC2/cc-pVTZ calculations.

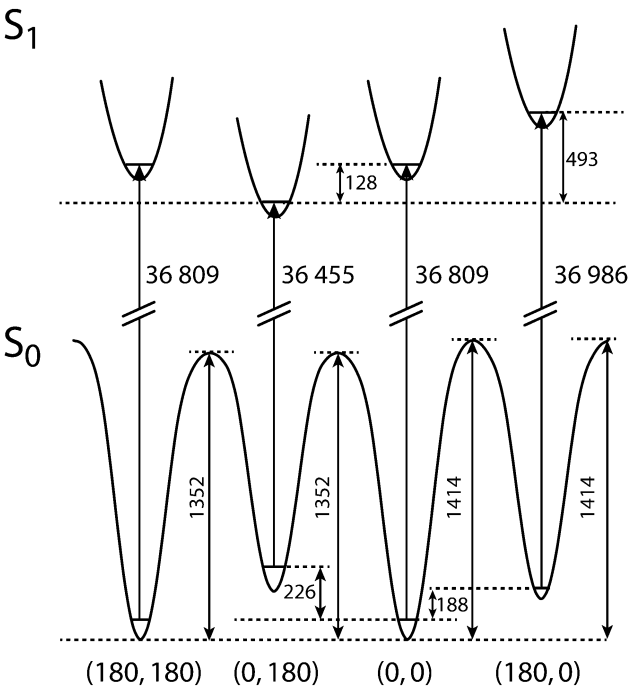

Fig. 3 Relative energies of the possible rotamers of 1,3-dimethoxybenzene according to CC2/cc-pVTZ calculations. All energies are given in cm^{-1}.

group along dihedral angle 2. Interchanging the order of rotation results in a path with the (180,0) rotamer as intermediate. Both paths follow saddle points, which are about 1400 cm^{-1} above the minimum structures. The direct (concerted) transition from (180,180) to (0,0) has the highest barrier of the three different

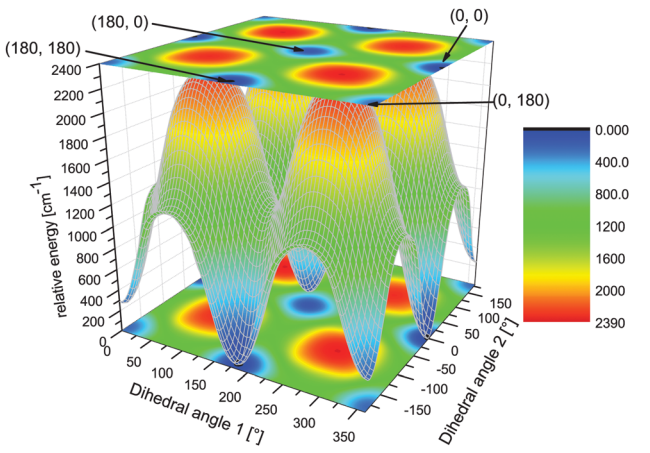

Fig. 4 Two-dimensional potential energy surface of 1,3-dimethoxybenzene in the ground state created by varying the dihedral angles of the substituents with respect to the aromatic plane in steps of 5° at DFT/B3LYP/cc-pVTZ level of theory.

paths with a value greater than 2300 cm^{-1} Thus, the motions can be treated in a one-dimensional manner; no cooperative effects of the rotations of both substituents are expected.

3.2 Experimental results

Fig. 5 shows the rotationally resolved spectrum of the electronic origin of the lowest energy band in the resonant two-photon ionization (R2PI) spectrum recorded by Yang *et al.*,[17] denoted as the A band. The spectrum of the second lowest energy band, denoted as the B band, is shown in Fig. 6. Both experimental spectra are accompanied by a simulation using the best parameters from a CMA-ES fit, given in Table 2. These include the rotational constants in the electronic ground (A'', B'', C'') and first electronically excited (A', B', C') states, the respective inertial defects (ΔI), the angle of the TDM vector with the inertial *a*-axis (θ), the excited state lifetime (τ) and the origin frequency (ν_0).

The electronic origins of both rotamers show a small deviation of less than one wavenumber compared to their low resolution values.[17] The A band is dominated by a-type transitions with less than 10% of b-type contributions. Hence, the TDM vector is almost parallel to the inertial *a*-axis and makes an angle of approximately 15° with it. For reasons of symmetry, which will be discussed in the next section, the θ angle of the B band was set to zero. The fit of the line shapes to Voigt profiles using a Gaussian (Doppler) contribution of 18 MHz yielded Lorentzian contributions of 13.1 ± 0.1 MHz for the A band and 9.4 ± 0.1 MHz for the B band. These line widths are equivalent to excited lifetimes of 12.1 ± 0.1 ns for the A and 17.0 ± 0.2 ns for the B band.

The C band, which was assigned by Yang *et al.*[17] to the origin of another rotamer, has a considerably smaller intensity than the A and B bands. The rovibronic spectrum of the C band is shown in Fig. S1, ESI.† The fit of this band resulted in the same

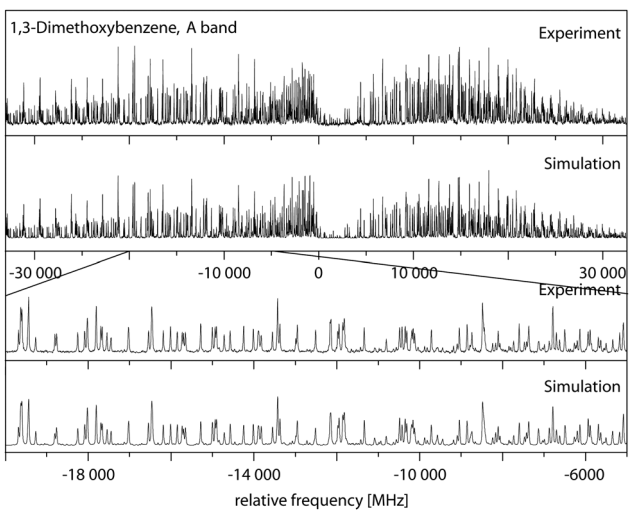

Fig. 5 Rotationally resolved spectrum of the electronic origin of the A band of 1,3-dimethoxybenzene, along with a simulation using the best CMA-ES fit parameters, given in Table 2. A modified version of this Figure with the residues of the fit is available in the ESI.†

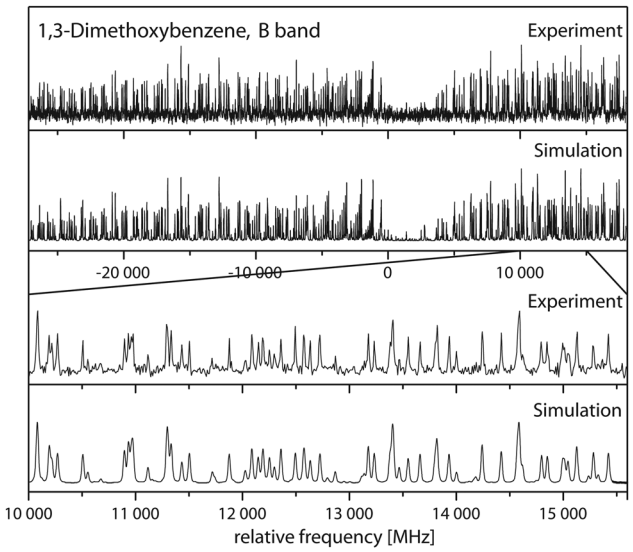

Fig. 6 Rotationally resolved spectrum of the electronic origin of the B band of 1,3-dimethoxybenzene, along with a simulation using the best CMA-ES fit parameters, given in Table 2. A modified version of this Figure with the residues of the fit is available in the ESI.†

Table 2 Molecular parameters obtained from a CMA-ES fit of the rovibronic spectra of three transition bands of 1,3-dimethoxybenzene. This includes the ground and excited state rotational constants. Double-primed constants belong to the ground state and single-primed to the excited state. The angle of the transition dipole moment with the main inertial axis *a* is given by θ and the adiabatic excitation energy by ν_0

	A band	B band	C band
A''/MHz	2533.44(45)	3461.98(360)	2533.17(60)
B''/MHz	887.52(2)	768.20(4)	887.41(12)
C''/MHz	663.11(2)	634.01(4)	663.04(7)
$\Delta I''$/μÅ^2	−6.78	−6.74	−6.79
A'/MHz	2477.65(45)	3338.30(360)	2483.22(61)
B'/MHz	875.60(3)	760.63(4)	873.59(13)
C'/MHz	652.93(3)	624.86(4)	653.61(8)
$\Delta I'$/μÅ^2	−7.14	−7.03	−8.8
ΔA/MHz	−55.80(1)	−123.68(1)	−49.96(4)
ΔB/MHz	−11.93(1)	−7.57(1)	−13.82(2)
ΔC/MHz	−10.18(1)	−9.15(1)	−9.44(2)
θ/°	±14.5(1)	0.0[a]	±12(2)
τ/ns	12.1(1)	17.0(1)	4.1(5)
ν_0/cm^{-1}	36117.61(2)	36185.72(1)	36268.75(10)

[a] For reasons of symmetry the angle was set to zero.

rotational constants as for the electronic ground state of the A band and slightly different rotational constants for the excited state. Thus, it is obvious that the C band is not the origin of another rotamer, as assumed by Yang *et al.*[17] and Breen *et al.*[16] They assigned the C band to the missing (0,180) rotamer. According to the present analysis, it can safely be assigned to a vibronic band, which is built on the A origin. The resulting molecular parameters are shown in Table 2.

3.3 Conformational assignment

While the vibrational frequencies of different rotamers are often quite similar, rotational constants or inertial moments

are extremely sensitive to conformational changes. As a consequence of this, even the slightest geometry changes can lead to dramatically different sets of rotational constants, especially if heavy atoms are involved. This can be seen from the calculated and experimental rotational constants of the different rotamers of 1,3-dimethoxybenzene in Tables 1 and 2. Going from rotamer (0,180) to (180,180)/(0,0), which is accompanied by a single rotation of a methyl group about 120°, leads to a change of around 700 MHz in the A'' and 200 MHz in the B'' constant. These changes are one third of the absolute values! Similar values are observed for a second rotation of the other methyl group, ending in rotamer (180,0). Since all rotamers are planar (at least in the electronic ground state) and the inertial *c*-axis is perpendicular to the aromatic plane, the rotational constant C remains almost unaffected by the geometry changes. However, each rotamer shows a characteristic set of rotational constants, which makes it possible to assign the observed bands to the respective structures.

Comparing the rotational constants of the experimental A and B band from Table 2 with the calculated values of all possible rotamers in Table 1, it becomes obvious that the A band belongs to rotamer (180,180)/(0,0) and the B band to rotamer (180,0), which is in agreement with the assignment made by Yang *et al.*[17] A direct comparison between the *ab initio* and experimental rotational constants is problematic, since the experimental constants are vibrationally averaged, while *ab initio* constants are equilibrium constants. In first approximation, vibrational averaging between rotamers of the same molecule is similar. Thus, the vibrational averaging effect cancels out in the difference of the rotational constants of different rotamers. The experimental A and B band have a difference of −931.56 MHz (−863.67 MHz) in the A'' (A'), +119.31 MHz (+114.96 MHz) in the B'' (B') and +29.11 MHz (+28.68 MHz) in the C'' (C') rotational constant. This fits well with the deviations of the rotational constants of the (180,180/0,0) and the (180,0) rotamer, which are −947 MHz (−876 MHz) for A'' (A'), +122 MHz (+117 MHz) for B'' (B') and +30 MHz (+29 MHz) for C'' (C'). This enables us to assign the A band to rotamer (180,180/0,0) and the B band to rotamer (180,0).

A further confirmation of this assignment comes from the comparison of the calculated and experimental adiabatic excitation energies. The electronic origin of the A band shows a redshift of 68 cm^{-1} compared to that of the B band. The combination of rotamers (180,180)/(0,0) and (180,0) exhibit a calculated red shift of 177 cm^{-1} while the electronic origin of rotamer (0,180) is redshifted by more than 300 cm^{-1}.

4 Discussion

The first question that we address is the planarity of the rotamers observed for 1,3-dimethoxybenzene in both electronic states. The inertial defect§ of the planar singly methoxy substituted benzene (anisole) in the ground state has been determined to −3.409 μÅ^2 using microwave spectroscopy[37] and to −3.584 μÅ^2 in the lowest excited singlet state by rotationally resolved laser induced fluorescence spectroscopy.[38] The experimentally determined inertial defect for the A rotamer (180,180)/(0,0) is −6.78 μÅ^2 for the electronic ground state and −7.14 μÅ^2 for the electronically excited state. For the B rotamer (180,0), −6.74 and −7.03 μÅ^2 are found. These values are slightly less than twice the inertial defect of anisole in its respective states. The larger inertial defect in the excited state points to an increased contribution of out-of-plane vibrations, as in the case of anisole. From the point of view of the inertial defects, both rotamers have a planar heavy atom structure.

Changing the methoxy group to a hydroxy group results in a planar structure with an inertial defect of −0.031 and −0.18 μÅ^2 in the lowest two singlet states of phenol.[39] The same holds true for the two experimentally observed rotamers of 1,3-dihydroxybenzene (180,180)/(0,0) and (180,0), with inertial defects close to zero in both states.[11,14]

For the mixed molecule 1-hydroxy-3-methoxybenzene, the three experimentally observed rotamers (180,180), (0,0) and (180,0) possess equally planar heavy atom structures in both states. This can be inferred from their inertial defects of −3.50, −3.46, and −3.47 μÅ^2 in the electronic ground and −3.80, −3.75 and −3.73 μÅ^2 in the lowest electronically excited state.[15]

However, for the fourth possible rotamer of 1-hydroxy-3-methoxybenzene (0,180), theory predicts a non-planar structure in the lowest electronically excited state, which is the reason for its absence in molecular beam studies due to a vanishingly small Franck–Condon factor for the origin excitation.[15] Looking at the calculated inertial defects of 1,3-dimethoxybenzene in Table 1 shows that the excited state value of the (0,180) rotamer is higher by more than 1 μÅ^2 compared to the other rotamers. This is caused by puckering of the hydrogen atom at C(2) out of the aromatic plane by 24°. In order to evaluate this effect, Franck–Condon simulations of the excitation spectra of all possible conformers of 1,3-dimethoxybenzene have been calculated and are summarized in Fig. 7. They have been obtained from the *ab initio* optimized ground and excited state structures of each rotamer and the respective Hessian using the program FCFit,[40,41] which computes the excitation spectrum in the FC approximation in the basis of multidimensional harmonic oscillator wavefunctions. While the excitation spectra of the (180,0) and (180,180)/(0,0) rotamers are quite similar, with only a few vibronic bands with significant intensities, most of the oscillator strength of the (0,180) rotamer is distributed over higher vibronic levels. Consequently, the Franck–Condon factor for the origin excitation of the (0,180) rotamer is dramatically smaller than for the other rotamers.

Table 3 summarizes the adiabatic and vertical excitation energies for all rotamers at CC2/cc-pVTZ level of theory. Inspection of the vertical excitation energies, calculated at the optimized ground state geometry, and comparing them to the one at the optimized excited state geometry, shows that the difference for rotamer (0,180) is almost twice that of the other rotamers. This confirms that the geometry change upon excitation is considerably larger for this rotamer. Although rotamer (0,180) is the most unstable in the ground state, its energy differs by less than 250 cm^{-1}

§ The inertial defect is defined as $I_c - I_a - I_b$, where the I_g are the moments of inertia with respect to the main inertial axes g of the molecule.

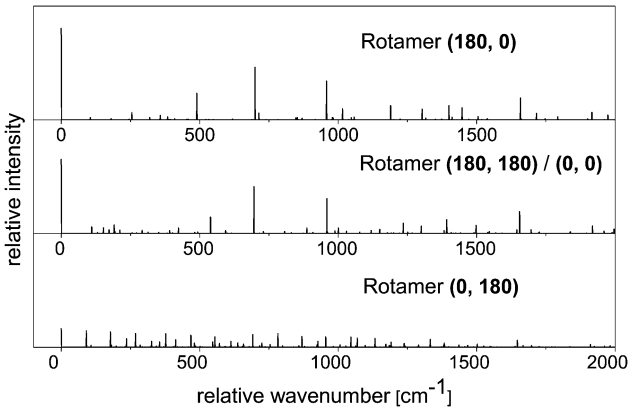

Fig. 7 Franck–Condon simulations of the excitation spectra of the possible rotamers of 1,3-dimethoxybenzene at CC2/cc-pVTZ level of theory. The individual spectra are normalized to the total area of all bands within this spectrum.

Table 3 Summary of different excitation energies of the 1,3-dimethoxybenzene rotamers at CC2/cc-pVTZ level of theory. All energies are given in cm^{-1}

	(180,180)/(0,0)	(180,0)	(0,180)
$\Delta E_{adiabatic}$ incl. ZPE	36 809	36 986	36 455
$\Delta E_{adiabatic}$ excl. ZPE	38 334	38 428	37 837
$\Delta E_{vertical}$ @ opt. S_0 geometry	39 807	39 728	39 476
$\Delta E_{vertical}$ @ opt. S_1 geometry	36 784	37 059	34 546

compared to the most stable one. Thus, it is unlikely that one of the rotamers is not populated thermally prior to expansion. Additionally, the barrier heights from Fig. 3 and the potential energy surface, given in Fig. 4, rule out the possibility of a depopulation of one rotamer into another. Therefore, the small Franck–Condon factor seems to be the most plausible explanation for the absence of rotamer (0,180) in our experiments.

A similar assumption based on intensities has already been made by Yang *et al.*,[17] where the origin peak of the most intense band (A) assigned to the (180,180)/(0,0) rotamer is observed to be more than ten times higher than the one of band C, which they assigned to the rotamer (0,180). However, in both experiments from Breen[16] and Yang[17] the band, that they assign to the electronic origin of rotamer (0,180) lies at the highest energy, while our CC2-calculations predict the lowest excitation energy compared to the other rotamers. The inertial parameters of the C band, which we obtained from the analysis of the rovibronic spectrum in the present study, clearly shows that the C band is a vibronic band belonging to the A origin. Thus, the origin of the (0,180) still remains undetected.

In order to explain this observation, a natural bond orbital (NBO) analysis has been performed. In general, the methoxy group is a mesomeric donating substituent which increases the electron density inside the chromophore. As was already observed for 5-hydroxyindole[42] and various conformers of serotonin,[43] there exists a conformation-dependent shift of electron density from the substituent to the chromophore depending on the orientation of the oxygen lone-pair with respect to the chromophore.

Table 4 Natural charges from a natural population analysis (NPA) for all possible rotamers of 1,3-dimethoxybenzene using the CC2/cc-pVTZ wave functions. For atomic labeling see Fig. 1. The bold marked values designate the atomic positions where the natural charges (or differences of natural charges) are highest

	(180,180)/(0,0)			(180,0)			(0,180)		
	q_{S_0}	q_{S_1}	Δq	q_{S_0}	q_{S_1}	Δq	q_{S_0}	q_{S_1}	Δq
C1	0.32	0.29	−0.03	0.31	0.28	−0.03	0.32	0.29	−0.03
C2	**−0.35**	**−0.42**	**−0.07**	−0.30	**−0.36**	**−0.07**	**−0.40**	**−0.48**	**−0.09**
C3	0.31	0.28	−0.04	0.31	0.28	−0.03	0.32	0.29	−0.03
C4	−0.27	−0.21	0.06	**−0.32**	−0.24	0.08	−0.27	−0.19	0.08
C5	−0.16	**−0.28**	**−0.11**	−0.16	**−0.27**	**−0.11**	−0.17	−0.29	**−0.12**
C6	**−0.33**	−0.23	−0.10	**−0.32**	−0.24	0.08	−0.27	−0.19	0.08
O7	−0.47	−0.43	0.05	−0.47	−0.43	0.05	−0.47	−0.43	0.05
O8	−0.47	−0.43	0.05	−0.47	−0.43	0.05	−0.47	−0.43	0.05
C9	−0.21	−0.21	−0.01	−0.21	−0.21	−0.01	−0.21	−0.21	−0.01
C10	−0.21	−0.21	0.00	−0.21	−0.21	−0.01	−0.21	−0.21	−0.01
H2	0.22	0.22	0.00	0.22	0.22	0.00	0.21	0.20	−0.01
H4	0.21	0.20	−0.01	0.21	0.20	−0.01	0.21	0.20	−0.01
H5	0.20	0.20	0.00	0.20	0.20	0.00	0.20	0.20	0.00
H6	0.21	0.20	−0.01	0.21	0.20	−0.01	0.21	0.20	−0.01
H9.1	0.18	0.18	0.00	0.18	0.18	0.00	0.18	0.18	0.00
H9.2	0.16	0.17	0.01	0.16	0.16	0.01	0.16	0.17	0.01
H9.3	0.16	0.17	0.01	0.16	0.16	0.01	0.16	0.17	0.01
H10.1	0.18	0.18	0.00	0.18	0.18	0.00	0.18	0.18	0.00
H10.2	0.16	0.17	0.01	0.16	0.16	0.01	0.16	0.17	0.01
H10.3	0.16	0.17	0.01	0.16	0.16	0.01	0.16	0.17	0.01

The negative charge is highest at the atom opposite to the lone pair. This is confirmed by the results of the NBO analysis in the ground state of the different 1,3-dimethoxybenzene rotamers, summarized in Table 4. Thus, inside the chromophore the electron density at C(2) and C(6) for rotamer (180,180)/(0,0), at C(4) and C(6) for rotamer (180,0), and at C2 for rotamer (0,180) has the highest value. In the electronically excited state the situation changes. For all rotamers, a shift of around 0.11 elementary charges from the substituents into the chromophore upon excitation was calculated. However, this mainly affects C(2) and C(5) where the natural charges become significantly negative compared to the respective ground state values. Since for rotamer (0,180), C(2) exhibits already an extremely negative charge in the electronic ground state, it becomes the most negative atom in the whole molecule in the excited state. As a consequence of this, the charges are no longer perfectly delocalized as is typical for most aromatic compounds. Thus, the chromophore of rotamer (0,180) loses its planarity in the excited state. In the ESI,† the dihedral angles inside the chromophore of the different rotamers of 1,3-dimethoxybenzene are given which confirm the planar structure for rotamer (180,180)/(0,0) and (180,0) and the non-planar structure for rotamer (0,180).

5 Conclusion

Two rotamers of 1,3-dimethoxybenzene were studied using rotationally resolved electronic spectroscopy and assigned to the (180,180)/(0,0) (A band) and (180,0) (B band) structure based on their rotational constants. Computational results of the conformational landscape reveal a planar structure for both rotamers, which is confirmed by the experimental inertial

defects. However, for the third possible rotamer (0,180), theory predicts a non-planar geometry in the lowest electronically excited state. The strong geometry change upon excitation results in a remarkably small FC-factor for the respective origin compared to that of the other rotamers and was not observed in our experiments. The band, which was assigned before by Breen and Yang[16,17] to this "missing" rotamer has clearly been shown to be due to a vibronic band of the (180,180)/(0,0) rotamer.

For closely related systems with two adjacent substituents (1,2-dimethoxybenzene, 1,2-dihydroxybenzene and 1-hydroxy-2-methoxybenzene), rotamer (0,180) is not a stable structure due to steric hindrance.[17,44–46] Nevertheless, this cannot be used as an argument for the respective meta-substituted systems because both methyl groups are around 500 pm away from each other. Thus, electronic effects have to be responsible for the absence of this rotamer. This has been proven for 1,3-dimethoxybenzene by NBO calculations, which show that the electron density at the C(2) ring carbon atom, located between the two methoxy groups, is considerably increased upon electronic excitation. This partial charge localization leads to a decrease in aromaticity and an out-of-plane puckering of the C(2) atom. Since the electronic ground state is planar, the FC factor for the origin is much smaller than for the other rotamers. Similar results have been observed for 1-hydroxy-3-methoxybenzene[15] and can be expected for 1,3-dihydroxybenzene. Also for these systems, rotamer (0,180) has not been observed experimentally in molecular beam studies although the energetic differences are small enough in the ground state to allow for thermal population, while the barriers between the rotamers are sufficiently high to avoid collisional relaxation into the lowest minimum at the PES.

The present study nicely shows the importance of molecular structural parameters in the determination of different rotamer or conformer structures. While the differences of inertial parameters (rotational constants) are large, different ionization potentials, different ion spectra and/or different vibrational spectra are not sufficiently sensitive to give a straightforward answer in these cases.

Acknowledgements

Financial support of the Deutsche Forschungsgemeinschaft *via* grant SCHM1043 12-3 is gratefully acknowledged. Computational support and infrastructure was provided by the "Center for Information and Media Technology" (ZIM) at the Heinrich-Heine-University Düsseldorf (Germany). We furthermore thank the Regional Computing Center of the University of Cologne (RRZK) for providing computing time on the DFG-funded High Performance Computing (HPC) system CHEOPS as well as support. Financial support provided by the Dirección de Apoyo a la Investigación y al Posgrado (DAIP)-Universidad de Guanajuato, under the grant CIFOREA 76/2016 is greatly appreciated. LAV acknowledges Dr. David Y. G. Delepine for his continue support for the establishment of the Molecular Spectroscopy High Resolution Laboratory in León, México. JTY acknowledges financial support *via* grant NSF RIA-1505311.

References

1 *Atomic and Molecular Beam Methods*, ed. G. Scoles, Oxford University Press, New York, Oxford, 1988, vol. 1.
2 *Atomic and Molecular Beam Methods*, ed. G. Scoles, Oxford University Press, New York, Oxford, 1992, vol. 2.
3 P. Felder and H. H. Günthard, *Chem. Phys.*, 1982, **71**, 9–25.
4 R. S. Ruoff, T. D. Klots, T. Emilsson and H. S. Gutowski, *J. Chem. Phys.*, 1990, **93**, 3142–3150.
5 P. D. Godfrey, R. D. Brown and F. M. Rogers, *J. Mol. Struct.*, 1996, **376**, 65–81.
6 T. Baer and A. R. Potts, *J. Phys. Chem. A*, 2000, **104**, 9397–9402.
7 M. Böhm, R. Brause, C. Jacoby and M. Schmitt, *J. Phys. Chem. A*, 2009, **113**, 448–455.
8 T. M. Dunn, R. Tembreull and D. Lubman, *Chem. Phys. Lett.*, 1985, **121**, 453–457.
9 C. Puebla and T.-K. Ha, *THEOCHEM*, 1990, **204**, 337–351.
10 M. Gerhards, W. Perl and K. Kleinermanns, *Chem. Phys. Lett.*, 1995, **240**, 506–512.
11 S. Melandri, G. Maccaferri, W. Caminati and P. G. Favero, *Chem. Phys. Lett.*, 1996, **256**, 513–517.
12 W. D. Geppert, C. E. H. Dessent, S. Ullrich and K. Müller-Dethlefs, *J. Phys. Chem. A*, 1999, **103**, 7186–7191.
13 W. D. Geppert, C. E. H. Dessent and K. Müller-Dethlefs, *J. Phys. Chem. A*, 1999, **103**, 9687–9692.
14 G. Myszkiewicz, W. L. Meerts, C. Ratzer and M. Schmitt, *ChemPhysChem*, 2005, **6**, 2129–2136.
15 M. Wilke, M. Schneider, J. Wilke, J. Ruiz-Santoyo, J. Campos-Amador, M. González-Medina, L. Álvarez-Valtierra and M. Schmitt, *J. Mol. Struct.*, 2017, **1140**, 59–66.
16 P. J. Breen, E. R. Bernstein, H. V. Secor and J. I. Seeman, *J. Am. Chem. Soc.*, 1989, **111**, 1958–1968.
17 S. C. Yang, S. W. Huang and W. B. Tzeng, *J. Phys. Chem. A*, 2010, **114**, 11144–11152.
18 S. Gerstenkorn and P. Luc, *Atlas du spectre d'absorption de la molécule d'iode 14800–20000 cm^{-1}*, CNRS, Paris, 1986.
19 M. Schmitt, *Habilitation*, Heinrich-Heine-Universität, Math. Nat. Fakultät, Düsseldorf, 2000.
20 M. Schmitt, J. Küpper, D. Spangenberg and A. Westphal, *Chem. Phys.*, 2000, **254**, 349–361.
21 R. Ahlrichs, M. Bär, M. Häser, H. Horn and C. Kölmel, *Chem. Phys. Lett.*, 1989, **162**, 165–169.
22 T. H. Dunning Jr., *J. Chem. Phys.*, 1989, **90**, 1007–1023.
23 C. Hättig and F. Weigend, *J. Chem. Phys.*, 2000, **113**, 5154–5161.
24 C. Hättig and A. Köhn, *J. Chem. Phys.*, 2002, **117**, 6939–6951.
25 C. Hättig, *J. Chem. Phys.*, 2002, **118**, 7751–7761.
26 P. Deglmann, F. Furche and R. Ahlrichs, *Chem. Phys. Lett.*, 2002, **362**, 511–518.
27 A. E. Reed, R. B. Weinstock and F. Weinhold, *J. Chem. Phys.*, 1985, **83**, 735–746.
28 TURBOMOLE V6.5 2013, a development of University of Karlsruhe and Forschungszentrum Karlsruhe GmbH, 1989–2007,

TURBOMOLE GmbH, since 2007, available from http://www.turbomole.com.

29 M. J. Frisch, G. W. Trucks, H. B. Schlegel, G. E. Scuseria, M. A. Robb, J. R. Cheeseman, G. Scalmani, V. Barone, B. Mennucci, G. A. Petersson, H. Nakatsuji, M. Caricato, X. Li, H. P. Hratchian, A. F. Izmaylov, J. Bloino, G. Zheng, J. L. Sonnenberg, M. Hada, M. Ehara, K. Toyota, R. Fukuda, J. Hasegawa, M. Ishida, T. Nakajima, Y. Honda, O. Kitao, H. Nakai, T. Vreven, J. A. Montgomery, Jr., J. E. Peralta, F. Ogliaro, M. Bearpark, J. J. Heyd, E. Brothers, K. N. Kudin, V. N. Staroverov, R. Kobayashi, J. Normand, K. Raghavachari, A. Rendell, J. C. Burant, S. S. Iyengar, J. Tomasi, M. Cossi, N. Rega, J. M. Millam, M. Klene, J. E. Knox, J. B. Cross, V. Bakken, C. Adamo, J. Jaramillo, R. Gomperts, R. E. Stratmann, O. Yazyev, A. J. Austin, R. Cammi, C. Pomelli, J. W. Ochterski, R. L. Martin, K. Morokuma, V. G. Zakrzewski, G. A. Voth, P. Salvador, J. J. Dannenberg, S. Dapprich, A. D. Daniels, Ö. Farkas, J. B. Foresman, J. V. Ortiz, J. Cioslowski and D. J. Fox, *Gaussian 09 Revision E.01*, Gaussian Inc., Wallingford CT, 2009.

30 W. L. Meerts, M. Schmitt and G. Groenenboom, *Can. J. Chem.*, 2004, **82**, 804–819.

31 W. L. Meerts and M. Schmitt, *Phys. Scr.*, 2005, **73**, C47–C52.

32 W. L. Meerts and M. Schmitt, *Int. Rev. Phys. Chem.*, 2006, **25**, 353–406.

33 M. Schmitt and W. L. Meerts, *Handbook of High Resolution Spectroscopy*, John Wiley and Sons, 2011.

34 A. Ostermeier, A. Gawelcyk and N. Hansen, *Parallel Problem Solving from Nature, PPSN III*, Springer, Berlin/Heidelberg, 1994.

35 N. Hansen and A. Ostermeier, *Evolutionary Computation*, 2001, **9**, 159–195.

36 C. Agache and I. V. Popa, *Monatshefte für Chemie/Chemical Monthly*, 2006, **137**, 55–68.

37 O. Desyatnyk, L. Pszczolkowski, S. Thorwirth, T. M. Krygowski and Z. Kisiel, *Phys. Chem. Chem. Phys.*, 2005, **7**, 1708–1715.

38 J. W. Ribblett, W. E. Sinclair, D. R. Borst, J. T. Yi and D. W. Pratt, *J. Phys. Chem. A*, 2006, **110**, 1478–1483.

39 G. Berden, W. L. Meerts, M. Schmitt and K. Kleinermanns, *J. Chem. Phys.*, 1996, **104**, 972–982.

40 D. Spangenberg, P. Imhof and K. Kleinermanns, *Phys. Chem. Chem. Phys.*, 2003, **5**, 2505–2514.

41 R. Brause, M. Schmitt, D. Spangenberg and K. Kleinermanns, *Mol. Phys.*, 2004, **102**, 1615–1623.

42 O. Oeltermann, C. Brand, M. Wilke and M. Schmitt, *J. Phys. Chem. A*, 2012, **116**, 7873–7879.

43 M. Wilke, C. Brand, J. Wilke and M. Schmitt, *Phys. Chem. Chem. Phys.*, 2016, **18**, 13538.

44 J. T. Yi, J. W. Ribblett and D. W. Pratt, *J. Phys. Chem. A*, 2005, **109**, 9456–9464.

45 T. Bürgi and S. Leutwyler, *J. Chem. Phys.*, 1994, **101**, 8418.

46 J. A. Ruiz-Santoyo, M. Rodríguez-Matus, J. L. Cabellos, J. T. Yi, D. W. Pratt, M. Schmitt, G. Merino and L. Álverez-Valtierra, *J. Chem. Phys.*, 2015, **143**, 094301.

